Sustained-release and pH-adjusted alginate microspheres-encapsulated doxorubicin inhibit the viabilities in hepatocellular carcinoma-derived cells

Cheng-Tang Pan[1,2,#], Ruei-Siang Yu[3,#], Chih-Jung Yang[2], Lih-Ren Chen[4,5], Zhi-Hong Wen[6], Nai-Yu Chen[1], Hsin-You Ou[7], Chun-Yen Yu[7,*], Yow-Ling Shiue[1,8,*]

[1]Institute of Precision Medicine, National Sun Yat-sen University, Kaohsiung, Taiwan
[2]Department of Mechanical and Electro-Mechanical Engineering, National Sun Yat-sen University, Kaohsiung, Taiwan
[3]Department of Pharmacy, Kaohsiung Armed Forces General Hospital, Kaohsiung, Taiwan
[4]Division of Physiology, Livestock Research Institute, Council of Agriculture, Tainan, Taiwan
[5]Department of Biotechnology and Bioindustry Sciences, National Cheng Kung University, Tainan, Taiwan
[6]Department of Marine Biotechnology and Resources, National Sun Yat-sen University, Kaohsiung, Taiwan
[7]Liver Transplantation Program and Departments of Diagnostic Radiology and Surgery, Kaohsiung Chang Gung Memorial Hospital, and Chang Gung University College of Medicine, Kaohsiung, Taiwan
[8]Institute of Biomedical Sciences, National Sun Yat-sen University, Kaohsiung, Taiwan

Running title: pH-adjusted alginate microspheres inhibit cell viability

[#]These authors contributed equally
[*]Correspondence:
Chun-Yen Yu, MD, email: y7192215@ms17.hinet.net
Yow-Ling Shiue, PhD, email: shirley@imst.nsysu.edu.tw

Keywords: sodium alginate; microsphere; ultrasonic atomization; Dox; pH-adjusted

Preprints (www.preprints.org) | NOT PEER-REVIEWED | Posted: 29 July 2021 doi:10.20944/preprints202107.0664.v1

Abstract

The objective of this study aimed to develop biodegradable calcium alginate microspheres carrying doxorubicin (Dox) at the micrometer-scale for sustained-release and the capacity of pH regulatory for transarterial chemoembolization. Ultrasonic atomization and $CaCl_2$ cross-linking technologies were used to prepare the microspheres. A 4 by 5 experiment was first designed to identify imperative parameters. The concentration of $CaCl_2$ and the flow rate of the pump were found to be critical to generate microspheres with a constant volume median diameter (~ 39 μm) across 5 groups with different alginate:$NaHCO_3$ ratios using each corresponding flow rate. In each group, the encapsulation efficiency was positively correlated to the Dox-loaded efficiency. Fourier-transform infrared spectroscopy showed that $NaHCO_3$ and Dox were step-by-step incorporated into the calcium alginate microspheres successfully. Microspheres containing alginate:$NaHCO_3$ = 1 exhibited rough and porous surfaces, high Young's modulus and hardness. In each group with the same alginate:$NaHCO_3$ ratio, the swelling rates of microspheres were higher in PBS containing 10% FBS compared to those in PBS alone. Microspheres with relative high $NaHCO_3$ concentrations in PBS containing 10% FBS maintained better physiological pH and higher accumulated Dox release ratios. In two distinct hepatocellular carcinoma-derived cell lines, treatments with microspheres carrying Dox demonstrated that the cell viabilities decreased in groups with relative high $NaHCO_3$ ratios in time- and dose-dependent manners. Our results suggested that biodegradable alginate microspheres containing relative high $NaHCO_3$ concentrations improved the cytotoxicity effects in vitro.

Preprints (www.preprints.org) | NOT PEER-REVIEWED | Posted: 29 July 2021 doi:10.20944/preprints202107.0664.v1

1. Introduction

Hepatocellular carcinoma (HCC) is one of the foremost cause of tumor-associated mortality worldwide and the incidence continues to increase [1]. Regrettably, HCC is usually diagnosed at intermediate or advanced stages while merely palliative remedies could be used, leading to a poor overall survival. Transarterial chemoembolization (TACE) is a frequently recommended treatment for asymptomatic, multifocal and/or large HCC devoid of macrovascular invasion or metastasis [2,3]. TACE intends to induce tumor neurosis, resulting in cytotoxic effects along with ischemia in the tumor tissue. Chemoembolization especially using Doxorubicin (Dox), improved the survival of stringently selected patients with unresectable hepatocellular carcinoma [2].

Numerous types of microspheres including temporary or permanent are commercially available for TACE. The most commonly used are DC Bead™ [4] and HapaSphere™ [3] with the major component of polyvinyl alcohol (PVA), which were approved by the Food and Drug Administration (FDA, USA), are biocompatible yet non-biodegradable [5]. The type and the size of the Dox-loaded microspheres decide drug release effects in vitro [6]. Thus, the fabrication of biodegradable microspheres to prevent permanent embolization, compress arterial walls and normal organs by drug-loaded agents, as well as postoperative complications, are extremely important. Several biodegradable and biocompatible polymers including gelatin [7], chitosan [8], chitooligosaccharide [9] and sodium alginate [10-12] have been reported to formulate microspheres for TACE. As a low-priced and non-toxic polyanionic polysaccharide, alginate, displays characteristics including highly biocompatible and hydrophilic, ease of gelation, inert nature, ease of availability and a feasible method of synthesis. Therefore, it an excellent choice for researchers to develop platforms for tissue engineering and drug delivery [13,14]. It is also frequently used as a viscosifier, stabilizer or gelling agent in food, textile, pharmaceutical and biotechnological industries [15]. Moreover, Dox-loaded alginate microspheres showed a delayed-release of drug in the liver, extending the function time and maintaining the Dox concentration after embolization [16].

An increase in the rate of glucose uptake and preferential production of lactate, even in the presence of oxygen, also known as the ‘Warburg Effect’ [17,18], is prevalent in human cancer [19]. Accordingly, the increase of intratumoral lactate and its secretion in the tumor microenvironment resulting in lactate acidosis becomes an essential element in cancer progression and treatment [20,21], including hepatocellular carcinoma [22]. Compared to the conventional methods to prepare microspheres, the water-based ion cross-linking technique

Preprints (www.preprints.org) | NOT PEER-REVIEWED | Posted: 29 July 2021 doi:10.20944/preprints202107.0664.v1

bestows distinguishing advantages. In order to fabricate alginate microspheres-encapsulated Dox with the spherical integrity for sustained-release, we previously used a dripping-cross-linking method to produce ~2 mm microspheres [11]. In this study, we aimed to promote the process to improve sustained-release Dox microspheres at a micrometer-scale, as well as to incorporate a pH-adjusting agent, $NaHCO_3$, for TACE.

2. Materials and Methods

2.1. Chemicals and reagents

Sodium alginate $(C_6H_7NaO_6)_n$, calcium chloride ($CaCl_2$) (Sigma-Aldrich, St. Louis, MO, USA), sodium bicarbonate ($NaHCO_3$) (J. T. Baker, Phillipsburg, NJ, USA), ethyl acetate ($CH_3COOCH_2CH_3$) (Merck, Darmstadt, Germany) and Dox (Concord Biotech Limited, Gujarat, India) were obtained. For cell culture, Dulbecco's Modified Eagle Medium (DMEM, for Huh-7 cells), Minimum Essential Medium (MEM, for Hep-3B cells) and antibiotics (10,000 IU/mL penicillin and 10,000 IU/mL streptomycin) were purchased from HyClone™ Laboratories Inc. (Logan, UT, USA). Fetal Bovine serum (FBS) and trypsin-EDTA were acquired from Gibco/Thermo Fisher Scientific (Carlsbad, CA, USA). All solutions were prepared with autoclaved Mini-Q ultrapure water. Solutions of sodium alginate, $CaCl_2$ (for cross-linking), $CH_3COOCH_2CH_3$ (the oil-phase solution) and Dox were prepared as 2.2 wt%, 7wt%, 10 wt% and 2 mg/mL, respectively.

2.2. Preparation of the Dox calcium alginate microspheres containing

The instruments including the infusion pump and height gage were used. A dripping-cross-linking method was applied to fabricate the calcium alginate microspheres. Supplementary Figure S1 displays the experimental setups where the mixture (sodium alginate, $NaHCO_3$ and Dox) was located in a syringe and the syringe was squeezed by an infusion pump (KDS100, kdScientific, Holliston, MA, USA). The ratios of sodium alginate to $NaHCO_3$ were designed as 8:1, 4:1, 2:1, 1:1 and 1:2. All solutions were prepared with sterilized Mini-Q ultrapure water. An ultrasonic atomization (8700-48H, Sono-Tek, Milton, NY, USA) with 43 kHz high-frequency vibrations (12 V and 0.56 A power output) was used to atomize the admixture into micron-sized droplets, dropped into the calcium chloride ($CaCl_2$) containing 10 wt% $CH_3COOCH_2CH_3$ (oil phase, to avoid aggregation) for cross-linking and continuously stirred for 3 h for solidification. Afterwards, the microspheres were collected by using a 10-micron/1500 mesh nylon filter (Shijiazhuang, Hebei, China), washed

Preprints (www.preprints.org) | NOT PEER-REVIEWED | Posted: 29 July 2021 doi:10.20944/preprints202107.0664.v1

with sterilized Mini-Q ultrapure water to remove extra ethyl acetate, sanitized with 75% ethanol for 10 min, rewashed with sterilized water and stored in $CaCl_2$ (0.6 wt%) solution at room temperature. All procedures were performed in a laminar flow hood.

2.3. Experimental design and analysis

Our previous study (Pan et al. 2020) identified 4 critical parameters impacting on the particle size of microspheres. Therefore, a 4 by 5 experiment was designed to identify the significance of each parameter to the particle size of the microspheres (Supplementary Table S1) and the code and level of all parameters were designated as Supplementary Table S2. A total of 17 experiments were performed to identify the significance of each parameter [the concentrations of sodium alginate and $CaCl_2$ (wt%), the stirring speed (rpm) and the flow rate of the pump (mL/h)]. For each experiment, one parameter was changed while others were fixed and experiment 1 served as the reference group (Supplementary Table S3). For each experiment, ≥ 3 independent trials were carried out to produce microspheres. An optical microscope (LV-UEPI, Nikon, Minato-ku, Tokyo, Japan) with MultiCam EZ M9 software (v2.2, BAITE, Kwun Tong, Kln., Hong Kong) was used to measure the particle diameters of 3 subset of the microspheres which were randomly sampled from each trail. The volume median diameter [Dv(50)] was next determined.

2.4. Drug encapsulation and loaded efficiencies

Exactly 10 mL of the Dox-loaded sodium alginate solution (2 mg/mL) was placed in a syringe to prepare the Dox-loaded microspheres. After the calcium alginate microspheres were fabricated, the remains of $CaCl_2$ solution and the Dox-loaded sodium alginate solution left in the syringe were collected and weighted. Drug residues in the syringe after dipping and gelation bath were both considered. The microspheres were dried at 65 °C overnight in an oven to remove the water. The encapsulation and loaded efficiencies were calculated with equations (1) and (2), where $W_{d,\,\text{total}}$, $W_{d,\,\text{residual}}$ and W_m are the total weight of Dox in the process, residual Dox in the syringe and cross-linking solution and the total weight of microspheres, respectively.

$$\textbf{Encapsulation efficiency (\%)} = \frac{W_{\text{d, total}} - W_{\text{d, residual}}}{W_{\text{d, total}}} \quad (1)$$

Preprints (www.preprints.org) | NOT PEER-REVIEWED | Posted: 29 July 2021 doi:10.20944/preprints202107.0664.v1

$$\textbf{Loaded efficiency (\%)} = \frac{W_{\text{d, total}} - W_{\text{d, residual}}}{W_{\text{m}}} \quad (2)$$

2.5. Characterization of the calcium alginate microspheres

2.5.1. Chemical and physical properties

The calcium alginate microspheres were designed to be applied as a hydrogel form. However, to evaluate their chemical and physical properties, microspheres were dried in an oven at 65 °C overnight for the following experiments. A Fourier-transform infrared spectroscopy (FTIR, Tensor 27IR, Bruker, Billerica, MA, USA) was used to obtain infrared spectra of the absorbance of distinct microspheres (before and after cross-linking, without or with $NaHCO_3$; without or with Dox). Dried microspheres were finely grounded with KBr (KBr:microshperes = 9:1) to prepare the pellets under the oil pressure of 15 MPa and the infrared spectra were scanned between 400 and 4000 cm^{-1}. The microscopic surface features of the calcium alginate microspheres were observed using a scanning electron microscope (SEM, JSM-6380, JEOL Ltd. Tokyo, Japan). Meanwhile, the acetone dispersion method was used to avoid the aggregation of microspheres. A nanoindenter (MST, Nano Indenter® XP, Oak Ridge, TN, USA) was utilized to examine the mechanical properties including Young's (elastic) modulus (Gpa) and hardness (Gpa). Alternatively, equivalent swelling studies of microspheres in the hydrogel form were performed in pH 7.4 and pH 6.5 PBS at 37 °C. This procedure was repeated until the microspheres reached a constant weight. All samples were prepared in triplicate. The swelling rates were calculated by equation (3), where *Wt* and *Wi* are the weight of swelled microspheres and the weight of initial microspheres.

$$\textbf{Swelling rate (\%)} = \frac{W_{\text{t}} - W_{\text{i}}}{W_{\text{i}}} \quad (3)$$

2.6. Analysis of the pH value in media and the drug release efficiency in vitro

A spectrophotometer (NANODROP 2000, ThermoFisher, Waltham, MA, USA) was used to measure Dox release. Since Dox shows a strong absorbance at wavelength 230 (Supplementary Figure S2A), a linear calibration curve was generated by series of dilutions with sterile MiniQ ultrapure water (0.0 to 0.4 mM) (Supplementary Figure S2B). Drug release efficiencies were measured in two solutions, PBS and PBS containing 10% FBS at 37 °C to simulate the medium of cell culture. The microspheres containing $NaHCO_3$ and Dox were prepared. All microspheres were washed three time with sterilized and Mini-Q ultrapure

Preprints (www.preprints.org) | NOT PEER-REVIEWED | Posted: 29 July 2021 doi:10.20944/preprints202107.0664.v1

water and the water was completely removed by suction. Literally, 2×10^5 microspheres were placed onto Millicell® hanging cell culture inserts (Merck KGaA, Darmstadt, Germany) in 48-well plates. Afterwards, 1.5 mL of PBS or PBS containing 10% FBS were individually added into the plates. Drugs were gradually released from the microspheres. At regular intervals, 1 μL of the supernatant from both the control and the Dox-loaded groups were sampled and analyzed using a NANODROP 2000. The drug release rate in each group was calculated using equation (4), where W_{dr} and W_{dm} are weight of drug release and the total weight of the drug in the microspheres. W_{dr} was calculated by OD_{230} using the calibration curve corresponding to the drug concentration and W_{dm} was estimated by the weight of 2×10^5 microspheres × the drug loaded rate.

$$\textbf{Drug releasing rate (\%)} = \frac{W_{\mathrm{dr}}}{W_{\mathrm{dm}}} \quad (4)$$

2.7. In vitro anticancer activities

Two HCC-derived cell lines Huh-7 and Hep-3B were used to evaluate the cell viabilities of the Dox-loaded microspheres compared to those without Dox. Cells were maintained in a humidified incubator with 5% CO_2 at 37 °C with DMEM and MEM containing 10% (v/v) FBS and 1% (v/v) antibiotics. Cells (6×10^4) were seeded in a 12-well plate overnight and treated with 5×10^4 microspheres (without or with the Dox) in the cell culture insert to specifically separate cells from the microspheres, yet containing sufficient media to cover the microspheres for drug release, as shown in Supplementary Figure S3A. This setup allowed the gradual release of Dox liberally circulating between the upper and lower chambers. Meanwhile, the wells without cells but with the same microspheres and medium were simultaneously prepared for the subsequent medium replacement to reach the cumulative Dox concentrations. Cells were collected after 4-, 8- and 12-day treatments and trypan blue exclusion assay was applied to analyze the cell viability using an automated cell counter (TC20, Bio-Rad, Hercules, CA, USA). Media with the cumulative Dox concentrations were replaced every 4 days to reduce the experimental errors due to the depletion of nutrients in the media. After cell viabilities were determined on days 4 and 8, the remaining unmeasured well plates were replaced with media without cells as shown in Supplementary Figure S3B. Those groups containing microspheres without Dox were subculture to 6×10^4 cells/well using the same medium.

Preprints (www.preprints.org) | NOT PEER-REVIEWED | Posted: 29 July 2021 doi:10.20944/preprints202107.0664.v1

2.8. *Statistics*

Statistical analyses were performed using SPSS software (Version 24, IBM, Armonk, NY, USA). One-way analysis of variance (ANOVA) was used to evaluate the significant differences of the cell viability among different groups, followed by a Scheffe multiple comparison test. To assess the effects of pH value, multiple regression analysis was applied. The drug release amount and pH value of the medium were the 'independent variables' while the cell viability was the 'dependent variable'. All continuous data are expressed as means ± SD. For each group, microspheres were prepared ≥ 3 repeats. A $p < 0.05$ is considered as statistical significance.

3. Results and Discussion

3.1. *The concentration of $CaCl_2$ and flow rate are critical for a constant volume median diameter*

Of 17 experimental groups, one-way ANOVA demonstrated the sum of squares (SS), degree of freedom (df), mean of square (MS), *F* test and *p* value of the Dv(50) between and within groups. No significant difference was found within groups for each parameter while significant differences were identified for the concentration of $CaCl_2$ (wt%) and flow rate (Table 1). The Dv(50) in all experiments are shown in Figure 1. Different concentrations of sodium alginate solution (Figure 1A) and stirring speeds (Figure 1C) produced Dox microspheres with Dv(50) of ~37.01 ± 1.09 to 44.03 ± 0.52 μm and ~38.75 ± 4.03 to 49.92 ± 3.65 μm . However, different concentrations of $CaCl_2$ and flow rates generated microspheres with Dv(50) of 32.00 ± 1.41 to 48.63 ± 4.48 μm and 29.50 ± 1.32 to 55.63 ± 7.06 μm, respectively. Post-hoc analysis further demonstrated that high $CaCl_2$ concentrations (7 to 11 wt%, $p < 0.05$, Figure 1B) and high flow rates of the pump (90 to 130 mL/h, $p < 0.05$, Figure 1D) increased the Dv(50) of microspheres. However, when the flow rate reached 170 mL/h, the Dv(50) of microspheres dropped to the size similar to that of 90 mL/h ($p < 0.05$, Figure 1D). These results suggested that the concentration of $CaCl_2$ and flow rate are critical parameters to engender the microspheres with a consistent Dv(50). On the other hand, parameters such as the concentration of sodium alginate solution and the stirring speed did not affect the Dv(50) in the ranges of 1.4 to 2.2 wt% and 100 to 300 rpm. Usually, low concentration of sodium alginate tends to form microspheres with the smaller particle size after cross-linking with $CaCl_2$[23]. The trend of relatively high sodium alginate concentration

Preprints (www.preprints.org) | NOT PEER-REVIEWED | Posted: 29 July 2021 doi:10.20944/preprints202107.0664.v1

resulted in higher Dv(50), consistent with the rationale but without statistical significance. On the other hand, we found that the Dv(50) gradually but non-significantly reduced, when the stirring speed increased. This phenomenon can be explained: high stirring rate causes atomized droplets to quickly exchange along the water flow into the cross-linking liquid at the bottom, reducing the likelihood of collision and fusion of the droplets after dripping and before cross-linking, thus reducing the particle size, which consists with earlier studies [24].

Table 1. The concentration of $CaCl_2$ and flow rate significantly affected the volume median diameter of calcium alginate microspheres

One-way ANOVA						
Parameters/variable		**SS**	**df**	**MS**	**F**	***p* value**
Sodium alginate solution (wt%)	Between Groups	153.077	4	38.269	0.893	0.473
	Within Groups	3084.728	72	42.843		
	Total	3237.805	76			
$CaCl_2$ solution (wt%)	Between Groups	800.926	4	200.232	5.916	0.000
	Within Groups	2436.879	72	33.846		
	Total	3237.805	76			
Stirring speed (rpm)	Between Groups	372.172	4	93.043	2.338	0.063
	Within Groups	2865.633	72	39.800		
	Total	3237.805	76			
Flow rate (mL/h)	Between Groups	1193.659	6	198.943	6.813	0.000
	Within Groups	2044.146	70	29.202		
	Total	3237.805	76			

SS: Sum of squares, **df**: Degree of freedom, **MS**: Mean square, **F**: F test

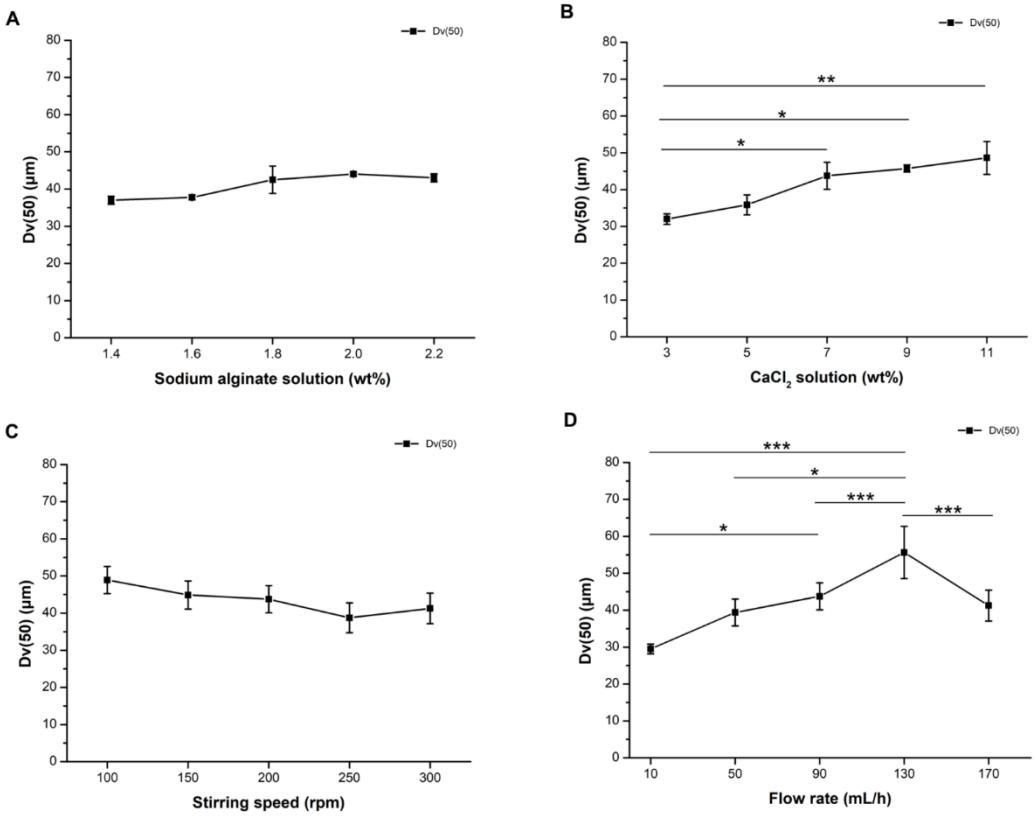

Preprints (www.preprints.org) | NOT PEER-REVIEWED | Posted: 29 July 2021 doi:10.20944/preprints202107.0664.v1

Figure 1. The concentration of $CaCl_2$ and flow rate are critical to fabricate alginate microspheres containing Dox with a consistent particle size. In order to obtain the most uniform median particle size of calcium-alginate microspheres, 4 parameters **(A)** concentration of sodium alginate (wt%), **(B)** concentration of $CaCl_2$ solution (wt%), **(C)** stirring speed (rpm) and **(D)** flow rate (mL/h) of the pump were screened. One-way ANOVA with post-hoc Scheffe multiple comparison indicated that the concentration of $CaCl_2$ solution and flow rate are the most critical factors among all. Dv(50): Median of diameter volume of the particle size. Statistical significance: $*p < 0.05$, $**p < 0.01$, $***p < 0.001$.

3.2. Optimization of the flow rate

To identify the optimal flow rate to generate microspheres with a coefficient of variation (CV, SD/mean) of Dv(50) < 5% , 5 groups with different alginate:$NaHCO_3$ ratios were prepared as Group 8:1, 4:1, 2:1, 1:1 and 1:2, and tested with different flow rates, 10, 30, 50, 90, 130 and 170 mL/h, respectively. The concentration of $CaCl_2$ was critical for Dv(50). We first fixed this at the middle value, 7 wt(%), because high $CaCl_2$ concentration inclines to form large Dv(50) [25]. The concentration of sodium alginate is not an imperative parameter (Table 1, Figure 1A), therefore, 2.2 wt%, the tolerable upper limit of the process was used across all groups. Besides, there was no significant Dv(50) differences among groups with different stirring speeds, and the speed was fixed at the middle value, 200 rpm (Figure 1C). After screening with different flow rates, Dv(50) ~39 μm with CV < 5% was found to be intersected across 5 groups (Figure 2), smaller to that (50 to 100 μm) of a commonly used commercial Hepasphere™ (V325HS, Biosphere Medical Rockland, MA, USA). Accordingly, the correspondent flow rates were 130, 90, 50, 30 and 10 mL/h for Group 8:1, 4:1, 2:1, 1:1 and 1:2, respectively (Table 2).

Figure 2 also shows the exact Dv(50) value in each group with a specific flow rate. In all groups, the Dv(50) steady increased as flow rates increase to 90 mL/h. Nevertheless, Dv(50) fluctuated in Groups 2:1 (alginate:$NaHCO_3$), 1:1 and 1:2 with relative high $NaHCO_3$ concentrations, when flow rates increased above 90 mL/h. The statistical significance between groups with a specific flow rate are shown in Supplementary Table S4. Briefly, Dv(50) was more diverse between groups at low flow rates (10, 30, 50 and 90 mL/h), while more close between groups at high flow rates (130 and 170 mL/h) with larger standard deviations. As the relative concentrations of $NaHCO_3$ increased, CO_2 gas was accumulated by dissolving Dox ($C_{27}H_{29}NO_{11}$·HCl) and $NaHCO_3$ in water and interfered with the process of ion cross-linking of alginate, similar to an earlier reports [2,26]. Furthermore, this system

Preprints (www.preprints.org) | NOT PEER-REVIEWED | Posted: 29 July 2021 doi:10.20944/preprints202107.0664.v1

effectively increases the Dv(50) at high flow rates, it also induced droplets by irregular atomization, comparable to previous findings [27].

Table 2. Optimization of the flow rate in five groups with different alginate:$NaHCO_3$ ratios to fabricate the microspheres with a consistent volume median diameter (~ 39 μm)

Alginate:$NaHCO_3$ (wt%:wt%)	Sodium alginate solution (wt%)	$CaCl_2$ solution (wt%)	Stirring speed (rpm)	[a]Optimized flow rate (mL/h)
8:1				130
4:1				90
2:1	2.2	7	200	50
1:1				30
1:2				10

[a]Flow rates: 10, 30, 50, 90, 130 and 170 mL/h, respectively, were tested

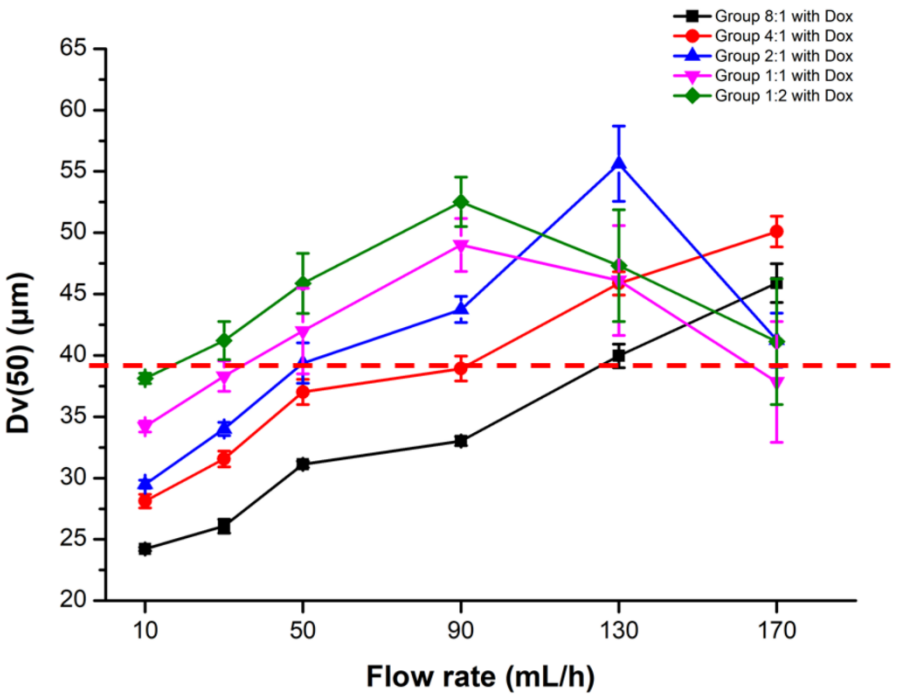

Figure 2. A volume median diameter [Dv(50)] of ~39.0 ± 1.95 μm coexisted in five groups with different alginate:$NaHCO_3$ ratios, determining the flow rate in each group for further experiments. Five groups of microspheres with different alginate:$NaHCO_3$ ratios were designed.

3.3. Dox encapsulation and Dox-loaded efficiencies

There are two TACE techniques that have been used since 2004, conventional TACE (cTACE) and TACE with drug-eluting beads (DEB-TACE). cTACE includes the intra-arterial injection of a chemotherapeutic drug (e.g., mitomycin C, cisplatin or Dox), which is

Preprints (www.preprints.org) | NOT PEER-REVIEWED | Posted: 29 July 2021 doi:10.20944/preprints202107.0664.v1

emulsified in the oily radio-opaque Lipiodol®, followed by intra-arterial injection of an embolic agent (gelatin sponge, polyvinyl alcohol particles or microspheres). Through cTACE, Lipiodol® carries the drug to tumor and induces microcirculation embolization [28,29]. Instead, DEB-TACE are non-resorbable embolic microspheres which can be loaded with a specific chemotherapeutic drug for more sustained drug release accompanying with embolization [30]. In this study, Dox encapsulation and loaded efficiencies of microspheres in 5 groups with different alginate:$NaHCO_3$ ratios (8:1, 4:1, 2:1, 1:1 and 1:2) along with its corresponding flow rate (Table 2) are shown in Figure 3A. The averages encapsulation and loaded efficiencies (%) of Group 8:1, 4:1, 2:1, 1:1 and 1:2 were estimated as 38.74% ± 1.70, 87.41% ± 1.71, 76.27% ± 1.78, 82.50% ± 3.40 and 75.93% ± 2.51, and 4.43% ± 0.19, 9.99% ± 0.20, 8.72% ± 0.20, 9.43% ± 0.39, 8.68% ± 0.29, respectively. In general, drug-loaded efficiencies were correlated to the encapsulation efficiencies across all groups. The encapsulation and loaded efficiencies reached the summit in Group 4:1 (alginate:$NaHCO_3$) with a flow rate of 90 mL/h compared to Group 1:2 with a flow rate of 10 mL/h ($p < 0.01$, Figure 3A). Representative images of the appearance of the microspheres from each group are shown in Figure 3B. Although the encapsulation and loaded efficiencies were similar among Group 2:1, 1:1 and 1:2, Group 1:2 exhibited fragmented microspheres compared to other groups, which may further affect Dox release, based on our previous study [11]. Moreover, a relative low $NaHCO_3$ concentration along with a high flow rate in Group 8:1, displayed poor encapsulation and loaded efficiencies. These may be also explained by irregular atomization droplets through high flow rates [27]. Therefore, Group 4:1, 2:1 and 1:1 (alginate:$NaHCO_3$) were subjected to further studies.

Preprints (www.preprints.org) | NOT PEER-REVIEWED | Posted: 29 July 2021 doi:10.20944/preprints202107.0664.v1

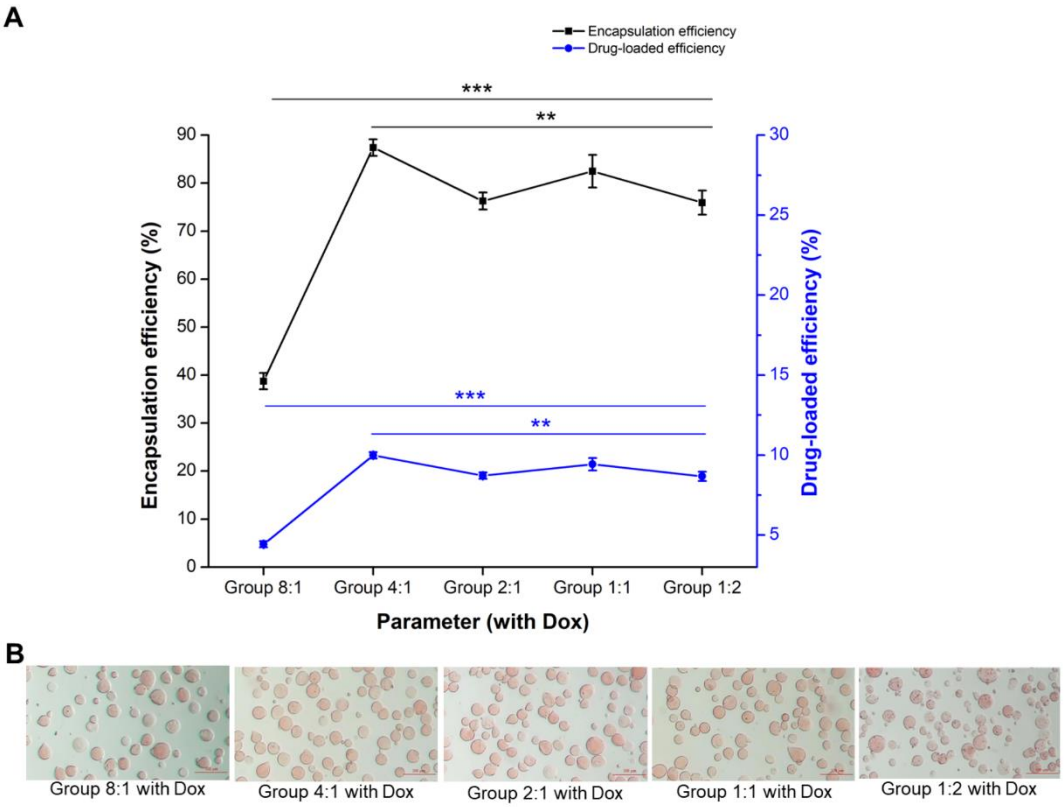

Figure 3. The Dox encapsulation and loaded efficiencies were similar in 3 among 5 groups with different alginate:$NaHCO_3$ ratios. **(A)** Encapsulation and loaded efficiencies. **(B)** An optical microscope showed the representative morphology of each group. Statistical significance: $^{**}p < 0.01$, $^{***}p < 0.001$. Bar scale = 100 μm.

3.4. The chemical and physical properties of alginate microspheres containing NaHCO3 and Dox

3.4.1. Chemical properties

Alterations of the chemical structure of sodium alginate and calcium alginate microspheres after cross-linking with $NaHCO_3$ were studied by a FTIR spectrum (Figure 4). Shifting of peaks (wavenumbers) were observed in calcium alginate microspheres by calcium cross-linking (Figure 4B) compared to sodium alginate power (Figure 4A), in calcium alginate microspheres containing $NaHCO_3$ through $NaHCO_3$ incorporation (Figure 4D) compared to calcium alginate microspheres (Figure 4B) and $NaHCO_3$ powder (Figure 4C) and in calcium alginate microspheres containing $NaHCO_3$ and Dox via Dox encapsulation (Dox-$NaHCO_3$, Figure 5F) compared to calcium alginate microspheres containing $NaHCO_3$ only (Figure 4D). This profile suggested that Dox-$NaHCO_3$ microspheres were step-by-step fabricated successfully.

Preprints (www.preprints.org) | NOT PEER-REVIEWED | Posted: 29 July 2021 doi:10.20944/preprints202107.0664.v1

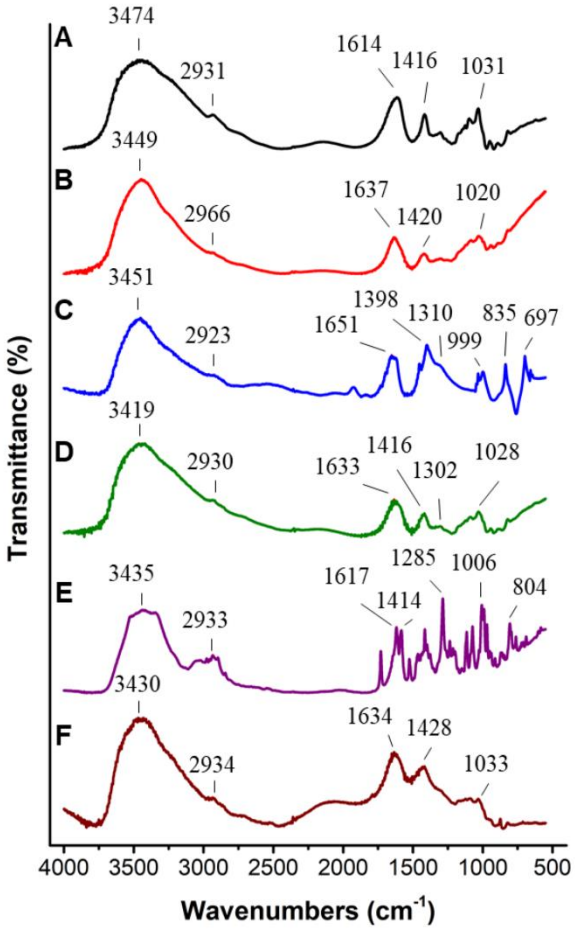

Figure 4. Fourier-transform infrared spectroscopy (FTIR) spectra of calcium alginate microspheres loaded with $NaHCO_3$ and Dox. **(A)** Sodium alginate power. **(B)** Calcium alginate microspheres. **(C)** $NaHCO_3$ powder. **(D)** Calcium alginate microspheres containing $NaHCO_3$ (B + C). **(E)** Dox. **(F)** **C**alcium alginate microspheres containing $NaHCO_3$ and Dox (D + E). Peaks shifting suggest Dox was successfully incorporated into calcium alginate microspheres containing $NaHCO_3$.

3.4.2. Physical properties

The surface microstructures of Dox/$NaHCO_3$ microspheres were observed using a SEM. Calcium alginate microspheres with Dox and different relative $NaHCO_3$ concentrations, Group 4:1 (alginate:$NaHCO_3$), 2:1 and 1:1 are shown in Figure 5 with different magnifications, 3000×, 5000×, 7000× and 9000× SEM identified that these microspheres shrunk due to the drying process and became irregular on their surfaces. Much smother surfaces were found in Group 4:1 with a relative low $NaHCO_3$ concentration (Figure 5A) compared to Group 2:1 (Figure 5B) and Group 1:1 (Figure 5C), since less CO_2 gas was accumulated when $NaHCO_3$ mixed with Dox in the process. Under 3000× magnification, the average diameter of Group 1:1 was larger compared to those of Group 2:1 and 4:1,

Preprints (www.preprints.org) | NOT PEER-REVIEWED | Posted: 29 July 2021 doi:10.20944/preprints202107.0664.v1

potentially due to low relative alginates in Group 1:1 was subjected to be dehydrated compared to Group 2:1 and 4:1.

Among 3 groups with different alginate:$NaHCO_3$ ratios, the Young's modulus (GPa) were similar between Group 2:1 (2.85 ± 0.07) and 1:1 (2.92 ± 0.12), higher than that of 4:1 (1.29 ± 0.09) ($p < 0.001$). Likewise, the hardness (GPa) was highest in Group 1:1 (0.11 ± 0.01) compared to those of 2:1 (0.08 ± 0.01; $p < 0.01$) and 4:1 (0.03 ± 0.00; $p < 0.001$). Also, the hardness of Group 2:1 was higher than that of Group 4:1 ($p < 0.001$) (Figure 6). These observations suggested that Group 1:1 retains both elasticity (to resist deformation) and hardness. Thus, in the presence of a same amount of Dox, the relative $NaHCO_3$ concentration is a critical factor to determine the elasticity and hardness (surface-to-mass ratio) of the alginate microspheres.

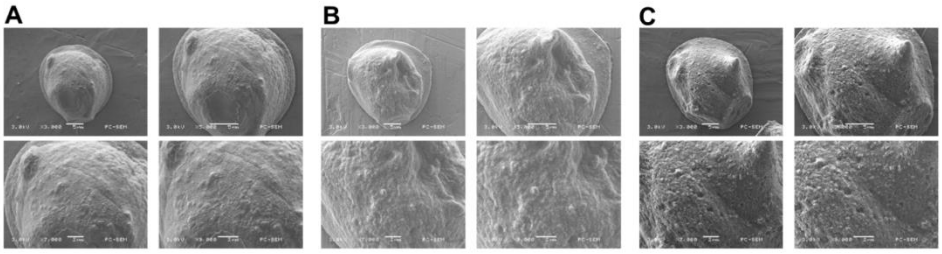

Figure 5. The surface microstructures of calcium alginate microspheres with different $NaHCO_3$ concentrations. A scanning electron microscope showed the surfaces of fabricated microspheres at 3000×, 5000×, 7000× and 9000× magnification. **(A)** Group 4:1 (Alginate:$NaHCO_3$), **(B)** Group 2:1 and **(C)** Group 1:1.

Preprints (www.preprints.org) | NOT PEER-REVIEWED | Posted: 29 July 2021 doi:10.20944/preprints202107.0664.v1

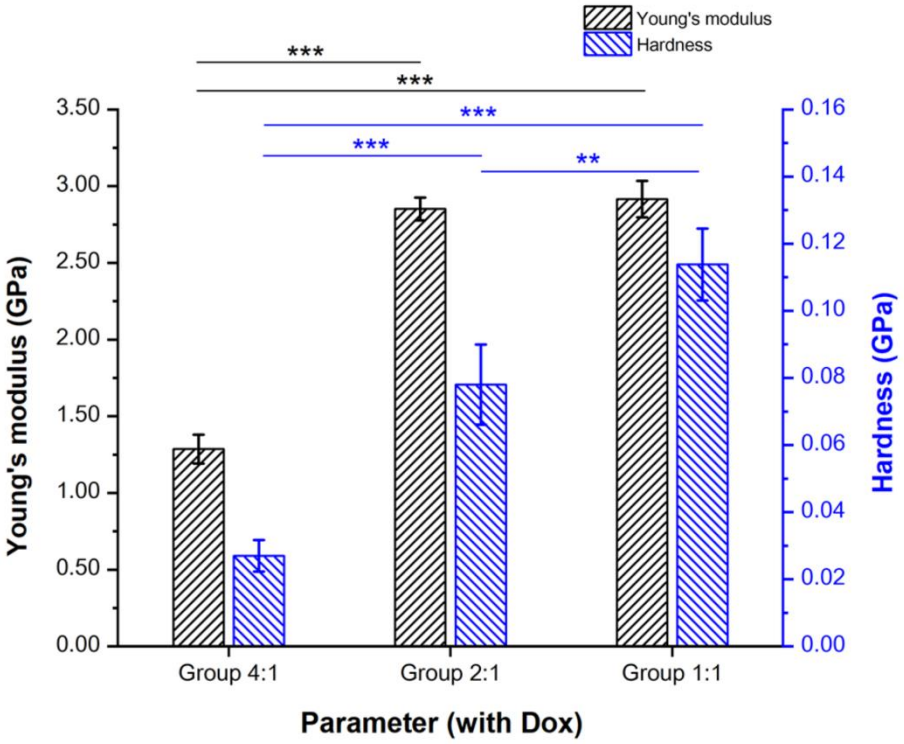

Figure 6. Microspheres with relative high $NaHCO_3$ concentrations resulted in higher Young's modulus and hardness. Among three groups with different alginate:$NaHCO_3$ (Group 4:1, 2:1 and 1:1), a nanoindenter identified their respective Young's modulus and hardness. Statistical significance: $^{**}p < 0.01$, $^{***}p < 0.001$.

3.4.3. *Swelling ratios of the Dox/NaHCO3 alginate microspheres in PBS with pH 7.4 and pH 6.5*

We prepared two PBS solutions with pH 7.4 (normal body fluids) and pH 6.5 (to mimic the tumor microenvironment), respectively, to measure the swelling rates of Dox/$NaHCO_3$ alginate microspheres at its hydrogel state from 0 to 24 h. After microspheres were immersed into PBS, the swelling ratios were rapidly increased during the first 30 min and gradually increased afterwards in all groups (alginate:$NaHCO_3$ = 4:1, 2:1 and 1:1, respectively, Figure 7). Swelling ratios can be clustered into two groups: pH 7.4 and pH 6.5 at 24 h after immersion in PBS. In general, microspheres with relative high $NaHCO_3$ concentrations showed higher swelling ratios in the same medium. The swelling rations of microspheres were much higher in pH 7.4 compared to those with pH 6.5 in Group 4:1 (4.23 ± 0.09 to 6.36 ± 0.25 vs. 1.41 ± 0.32 to 1.91 ± 0.16; $p < 0.001$), 2:1 (4.34 ± 0.16 to 6.64 ± 0.12 vs. 2.13 ± 0.13 to 2.96 ± 0.12; $p < 0.001$) and 1:1 (5.71 ± 0.15 to 7.81 ± 0.30 vs. 2.27 ± 0.15 to 3.83 ± 0.13; $p < 0.001$) from 0.5 h to 24 h (Supplementary Table S5). These observations, as

Preprints (www.preprints.org) | NOT PEER-REVIEWED | Posted: 29 July 2021 doi:10.20944/preprints202107.0664.v1

consisted to an earlier report, were due to the acidic condition that enhanced COOH formation and compacted the microsphere, while the alkaline condition on the other hand promoted Ca^{2+} binding to two COO- groups and relaxed the structure of microspheres [31]. At pH 6.5, the swelling rates were different in Group 4:1 (alginate:$NaHCO_3$) vs. 2:1 ($p < 0.01$), Group 4:1 vs. 1:1 ($p < 0.001$) and Group 2:1 vs. 1:1 ($p < 0.01$) after immersion into PBS for 0.5 to 24 h. Instead, at pH 7.4, due to similar swelling ratios between Group 4:1 and 2:1, higher swelling ratios were found in Group 4:1 vs. 1:1 ($p < 0.05$) and 2:1 vs. 1:1 ($p < 0.01$) after immersion in PBS for 0.5 h to 12 h (Supplementary Table S6). However, the significant difference was only retained in Group 4:1 vs. 1:1 after immersion in PBS for 24 h owing to the degradation (loss of weight and fragmentation) of the microspheres, resulting in large standard deviations (Figure 7). Accordingly, in pH 7.4 PBS, the microspheres absorbed PBS rapidly, and the swelling ratios reached up to ~7.37 ± 0.19 (Group 1:1) folds compared to ~3.83 ± 0.13 folds (Group 1:1) at 2 h in pH 6.5 PBS. The average swelling rate is larger than those of Hepaspheres™ in pH 7.4 PBS (~4 folds, 200 to 400 μm). Therefore, after multiplication of its original size, Dv(50) ~39 μm, Group 1 microspheres in pH 7.4 PBS can be expanded to ~287 μm. This Dv(50) falls into the diameter range of Hepaspheres™ after expansion, reinforcing that Dox/$NaHCO_3$ microspheres fabricated in this study are suitable for clinical usage.

Indeed, the sensitivity to pH value is one important feature of the calcium alginate microspheres. The swelling ratios were markedly suppressed under low pH environment. It has been reported that alginate-poly(γ-glutamic acid) composite microparticles could uptake hundreds of times of their weight in water. Both the maximum water uptake ratio and the swelling rate were increased by enlarging the amount of poly(γ-glutamic acid) in the composite [32]. Through the immersion of quercetin/chitosan/sodium alginate microspheres in PBS with 3 different pH values, simulated gastric fluid pH 1.2 and simulated intestinal fluid pH 6.8 and 7.4, the swelling index decreased as the pH value declined [33,34]. This phenomenon was potentially caused by acid conditions which protonated the carboxylate groups of the polymers on the surface of microspheres. Thus, the formation of hydrogen bonds with insoluble alginate in a low pH fluid increases the structure stability, hampering the diffusion of additional fluid into the core of each microsphere [34], consisting with the observations in our previous [11] and this study.

Preprints (www.preprints.org) | NOT PEER-REVIEWED | Posted: 29 July 2021 doi:10.20944/preprints202107.0664.v1

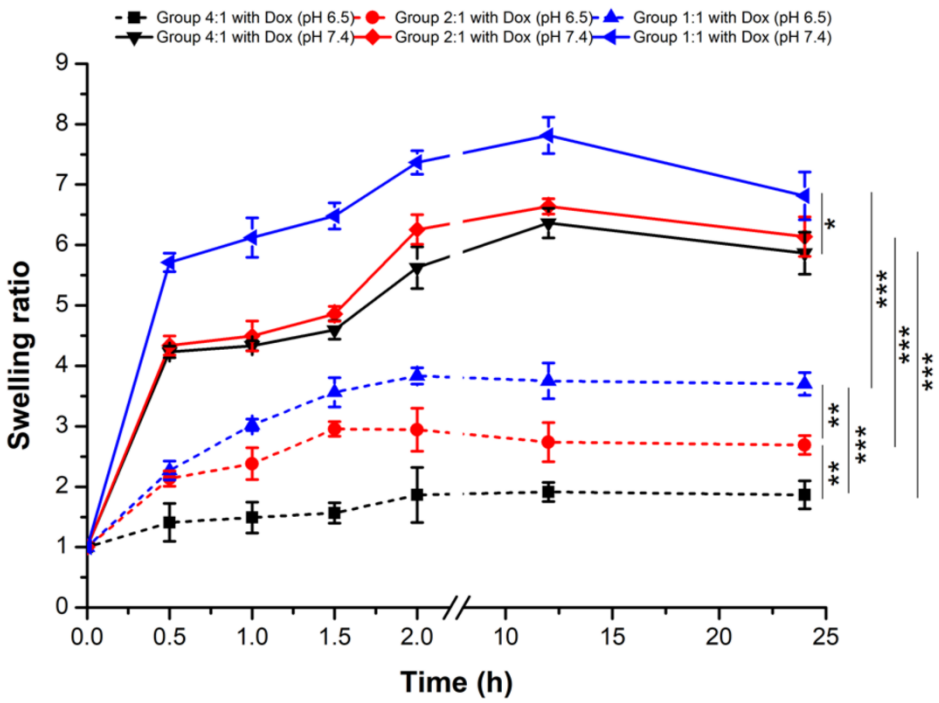

Figure 7. Higher swelling ratios in Dox-loaded microspheres in pH 7.4 PBS compared to pH 6.5 PBS across all group. Three different groups of microspheres with different alginate:$NaHCO_3$ were 4:1, 2:1 and 1:1, and swelling rates were measured by the weighting difference. Statistical significance: *$p < 0.05$, **$p < 0.01$, ***$p < 0.001$.

3.5. Relative high $NaHCO_3$ concentrations and 10% FBS enhance accumulated Dox release rates in PBS

The objective of adding 10% FBS to PBS was to simulate an environment of cell culture. The pH values in the media were measured in Figure 8A. In Group 4:1, 2:1 and 1:1 (alginate:$NaHCO_3$), the average pH values ranged from 6.87 ± 0.06 to 7.56 ± 0.05 in PBS while the average pH values ranged from 6.01 ± 0.06 to 8.16 ± 0.02 in PBS containing 10% FBS. Overall, the distribution of average pH values for Group 4:1, 2:1 and 1:1 were more centralized in PBS compared to those in PBS containing 10% FBS. From day 1 to day 22 after immersion, the pH values oscillated to some extent from microspheres across all groups in PBS as well as in PBS containing 10% FBS. At day 22, the average pH values in each group (4:1, 2:1 and 1:1, respectively) were different in PBS containing 10% FBS compared to those in PBS only ($p < 0.01$ to $p < 0.001$, Supplementary Table S7). The average pH values in Group 4:1 were always lower than those in Group 2:1 and 1:1, containing relatively higher $NaHCO_3$ concentrations in PBS and PBS with 10% FBS ($p < 0.01$, Figure 8A, Supplementary Table S8). In PBS containing 10% FBS, the average pH values suddenly

Preprints (www.preprints.org) | NOT PEER-REVIEWED | Posted: 29 July 2021 doi:10.20944/preprints202107.0664.v1

increased in Group 1:1 and abruptly decreased in Group 4:1 at day 22 compared to day 18, due to the disruption of microspheres (data not shown). Accordingly, in both PBS and PBS containing 10% FBS, Group 2:1 and 1:1 with relative high $NaHCO_3$ concentrations maintained better physiological PH values (~PH 7.4) compared to those of Group 4:1 with relative low $NaHCO_3$ concentrations.

Accumulated Dox release rates are shown in Figure 8B. In all groups, Dox released rapidly at day 1 and gradually released thereafter in PBS as well as PBS containing 10% FBS. Accumulated Dox release rates remained similar starting day 14 to day 22, reaching a plateau in each group. Dox release in PBS increased every 2-3 days in Group 4:1 (2.59% ± 0.27 to 11.61% ± 0.84), 2:1 (9.66% ± 0.74 to 14.66% ± 1.04) and 1:1 (12.22% ± 0.99 to 22.31% ± 1.61). Likewise, Dox release in PBS containing 10% FBS increased every 2-3 day in Group 4:1 (12.46% ± 0.28 to 27.53% ± 0.14), 2:1 (16.37% ± 0.60 to 31.46% ± 0.61) and 1:1 (18.92% ± 0.22 to 34.14% ± 0.84) (Figure 8B), i.e., accumulated release rates were higher in PBS containing 10% FBS compared to those in PBS only across all groups (4:1, 2:1 and 1:1, $p < 0.001$, Figure 8B; Supplementary Table S9), similar to our previous study [11]. FBS contains proteins/enzymes and unknown factors and destabilized the structure of alginate microspheres, potentially lead to faster drug release. At day 22, Dox release rates in Group 4:1 vs. 2:1 ($p = 0.04$, $p = 0.001$), 4:1 vs. 1:1 ($p < 0.001$, $p = 0.000$) and 2:1 vs. 1:1 ($p = 0.005$, $p = 0.005$) were different in PBS and PBS containing 10% FBS, respectively (Supplementary Table S10), i.e., higher relative $NaHCO_3$ concentrations resulted in more Dox releases. Low environmental pH comprises a high concentration of hydrogen ions binding to the carboxylic acid group in alginates, provoking further compacts of the microspheres to prevent swelling and drug releasing, consisting with earlier studies [31]. Accordingly, both FBS in the environmental media as well as relative high $NaHCO_3$ concentrations in microspheres enhance Dox release from the microspheres.

Preprints (www.preprints.org) | NOT PEER-REVIEWED | Posted: 29 July 2021 doi:10.20944/preprints202107.0664.v1

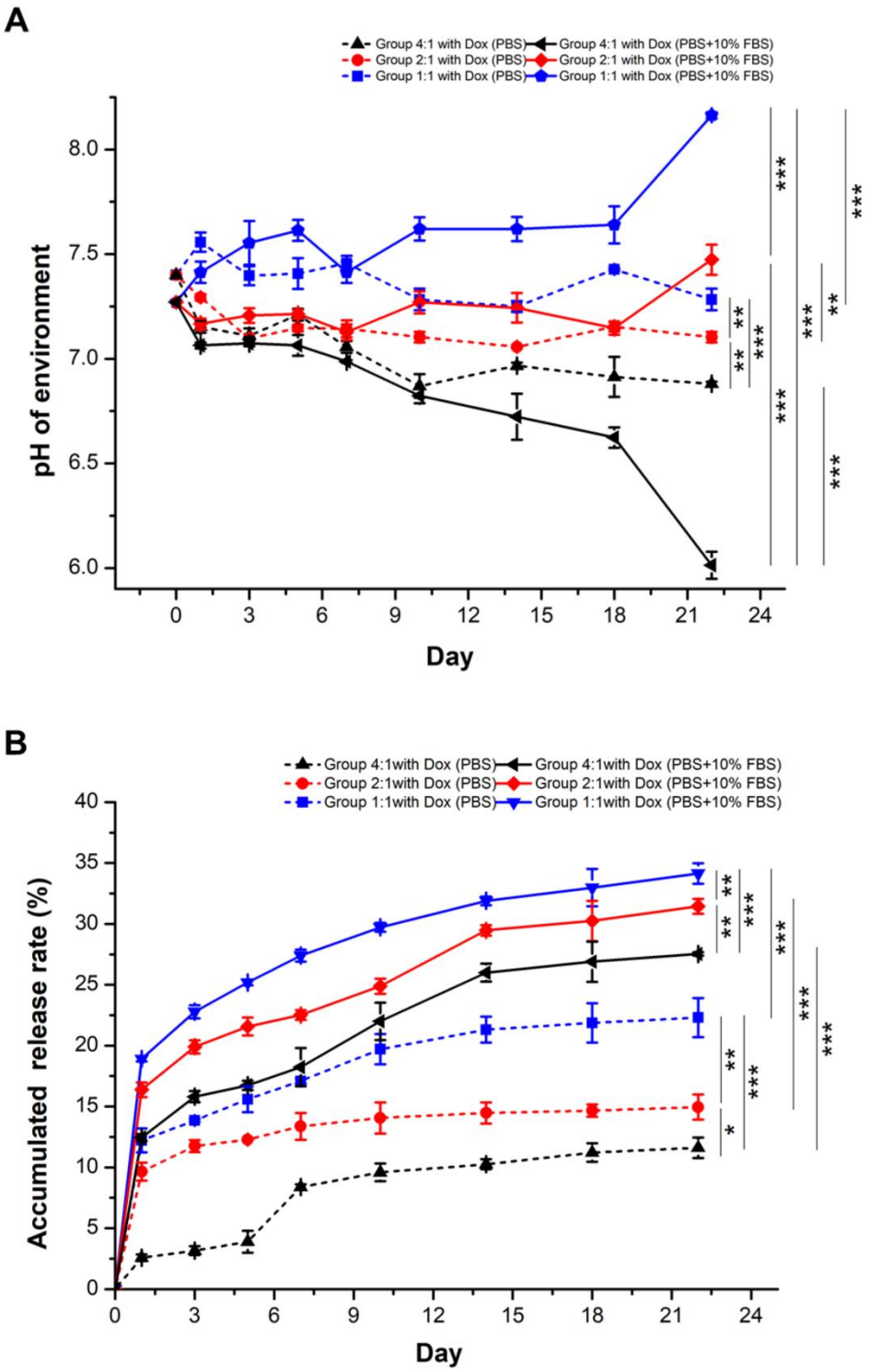

Figure 8. Alterations of the environmental pH values and Dox accumulated release rates after the immersion of the Dox-and $NaHCO_3$-loaded microspheres in pH 7.4 PBS and pH 6.5 PBS for 22 days. **(A)** A pH meter was used to measure the pH value. **(B)** Accumulated Dox release rates were measured using a NanoDrop spectrophotometer in different groups. Statistical significance: *$p < 0.05$, **$p < 0.01$, ***$p < 0.001$.

3.6. Alginate microspheres containing relative high $NaHCO_3$ concentrations strongly

Preprints (www.preprints.org) | NOT PEER-REVIEWED | Posted: 29 July 2021 doi:10.20944/preprints202107.0664.v1

inhibit cancer cell viabilities in vitro

Two hepatocellular carcinomas-derived cell lines, Huh-7 and Hep-3B with distinct genetic backgrounds, were used to evaluate the cytotoxicity of alginate microspheres with or without $NaHCO_3$ and/or with or without Dox. A total of 5 groups were designed: alginate microspheres (blank), alginate microspheres with $NaHCO_3$ (1:1) without Dox (control), Group 1:1 (alginate:$NaHCO_3$) with Dox, Group 2:1 with Dox and Group 4:1 with Dox. The cell morphologies of both cell lines were not changed after treatments with alginate microspheres (blank) from day 1 to day 12, while the cell densities were gradually increased with incubation time. Similar aspects were observed in the control group (alginate:$NaHCO_3$ = 1:1 without Dox). However, cell shrinkage was observed starting day 2 to day 12 in Group 4:1, 2:1 and 1:1 with Dox in Huh-7 (Figure 9A) and Hep-3B (Figure 9B) cells.

In both cell lines, the cell viabilities were quite stable between blank (Huh-7: 99.32% ± 0.50 to 99.03% ± 0.59; Hep-3B: 99.67% ±0.58 to 99.00 ± 0.47) and control (Huh-7: 99.00% ± 1.09 to 99.10% ± 0.92; Hep-3B: 99.33% ± 1.04 to 99.00% ± 0.99) after treatments with different microspheres for 4 to 12 days. Cell viabilities were stepwise decreased in Group 4:1 (Huh-7: 74.02% ± 0.89 to 55.33% ± 3.83, $p < 0.001$; Hep-3B: 83.50% ± 2.59 to 38.67% ± 1.86, $p < 0.001$), 2:1 (Huh-7: 61.50% ± 1.04 to 29.51% ± 1.15, $p < 0.01$; Hep-3B: 76.17% ± 3.06 to 26.36% ± 1.47, $p < 0.001$) and 1:1 (Huh-7: 25.50% ± 1.13 to 8.51% ± 1.05, $p < 0.001$; Hep-3B: 67.65% ± 1.63 to 14.14% ± 2.96, $p < 0.001$) compared those of blank and control after treatments for 4 to 12 days. Significant differences were observed in pairwise comparisons between every two groups after treatments for 4 days ($p < 0.01$), 8 days ($p < 0.001$) and 12 days ($p < 0.001$). Cell viabilities were likewise stepwise decreased within the same group after treatments for 12 days compared to those of 8 days ($p < 0.001$) and 4 days ($p < 0.001$), respectively; 8 days compared to that of 4 days ($p < 0.001$) (Figure 9C). Similar tendencies were found in Hep-3B cells, except for the decrease trends of cell viabilities were milder compared to those of Huh-7 cells (Figure 9D), owing to Hep-3B as a Tumor Protein 53 (*TP53*)-deficient cell line [35]. Resistance to TP53-mediated growth arrest and apoptosis in Hep-3B cells have been reported [36].

Multiple linear regression analysis with the model summary was next performed to evaluate whether Dox and/or pH affect the cell viabilities (Table 3). Supplementary Table S11 lists the model summary. In Huh-7 and Hep-3B cells, the R^2 values ranged from 0.723 to 0.975 and the adjusted R^2 values ranged from 0.686 to 0.972, across day 4, 8 and 12 after treatments with Dox/$NaHCO_3$-microspheres. These estimates indicated that the variable, i.e.,

Preprints (www.preprints.org) | NOT PEER-REVIEWED | Posted: 29 July 2021 doi:10.20944/preprints202107.0664.v1

the cell viability, can be highly explained by two independent variables, the Dox release amount and the environmental pH value. ANOVA next showed that the Dox release amount and the environmental pH impact on cell viabilities in both cell lines after treatments with Dox/$NaHCO_3$-microspheres for 4 days ($p < 0.001$), 8 days ($p < 0.001$) and 12 days ($p < 0.001$) (Supplementary Table S12). Multiple linear regression analysis showed negative standardized coefficients between the cell viabilities and the environmental pH as well as Dox releases after treatments with Dox/$NaHCO_3$/calcium alginate microspheres for 4, 8 and 12 days in both cell lines. Although Dox release slowed down after treatments with Dox/$NaHCO_3$-microspheres from day 4 to day 12 ($p = 0.025$ to $p = 0.874$), the environmental pH value continued to play an important role to inhibit cell viabilities ($p = 0.000$ to $p = 0.007$) in both cell lines (Table 3).

Table 3. Multiple linear regression analysis demonstrated that high environmental pH values reduced the cell viabilities after treatments with Dox/$NaHCO_3$/calcium alginate microspheres for 4, 8 and 12 days

Cells		Unstandardized Coefficient	Standardized Coefficient	*t* test	*p* value	VIF
Huh-7						
Day 4	Constant	1989.646		2.949	0.010	
	pH	-22.939	-0.531	-3.152	0.007	1.535
	Dox	-14551.143	-0.421	-2.499	0.025	1.535
Day 8	Constant	504.923		0.767	0.455	
	pH	-46.177	-0.938	-8.664	0.000	1.861
	Dox	-1043.472	-0.020	-0.185	0.856	1.861
Day 12	Constant	-104.376		-0.405	0.691	
	pH	-18.435	-1.022	-14.526	0.000	1.778
	Dox	-2076.344	-0.067	-0.956	0.354	1.778
Huh-3B						
Day 4	Constant	1309.960		2.630	0.019	
	pH	-25.373	-0.686	-4.723	0.000	1.535
	Dox	-8687.680	-0.293	-2.021	0.062	1.535
Day 8	Constant	343.403		1.480	0.160	
	pH	-33.141	-0.981	-17.648	0.000	1.861
	Dox	-319.867	-0.009	-0.161	0.874	1.861
Day 12	Constant	515.078		0.902	0.381	
	pH	-21.376	-0.894	-7.606	0.000	1.778
	Dox	-2753.621	-0.067	-0.572	0.576	1.778

Dox: Dox release amount (μg), **VIF:** variance inflation factor

Preprints (www.preprints.org) | NOT PEER-REVIEWED | Posted: 29 July 2021 doi:10.20944/preprints202107.0664.v1

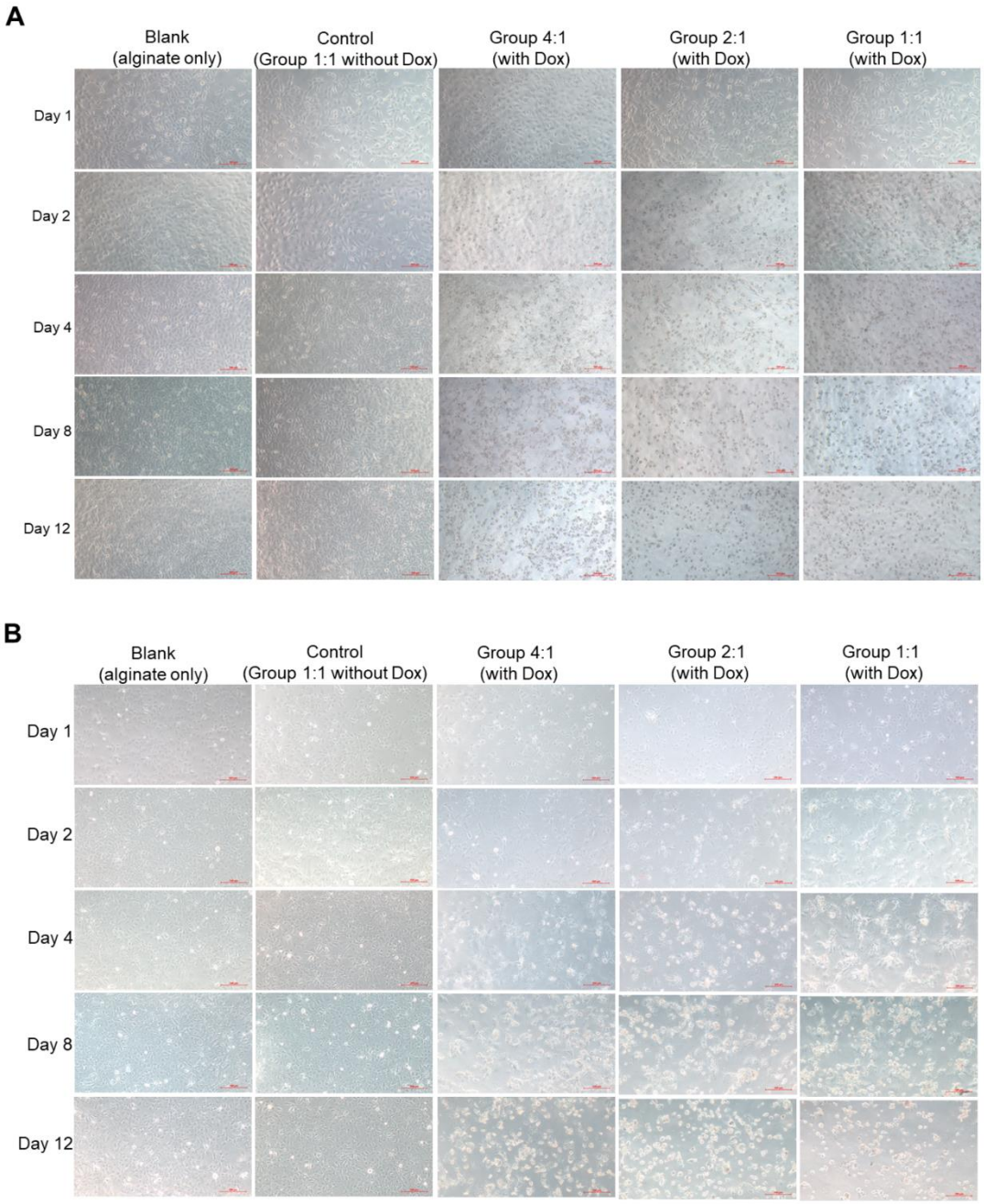

Preprints (www.preprints.org) | NOT PEER-REVIEWED | Posted: 29 July 2021 doi:10.20944/preprints202107.0664.v1

C

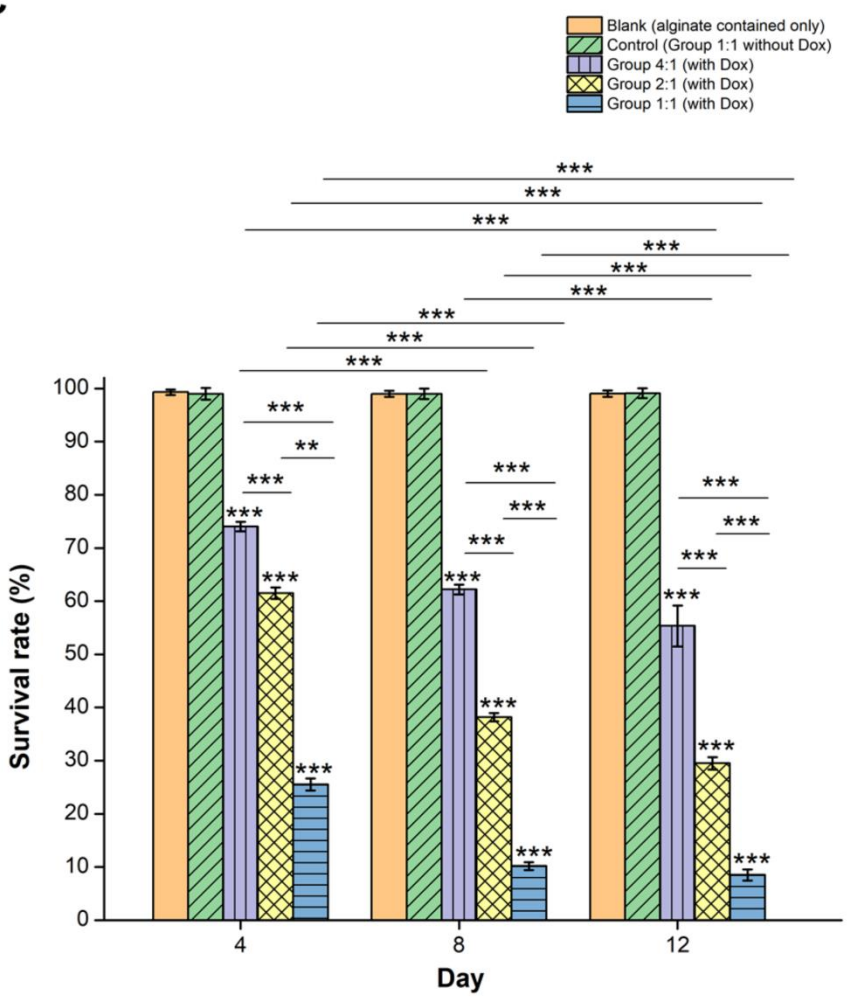

Preprints (www.preprints.org) | NOT PEER-REVIEWED | Posted: 29 July 2021 doi:10.20944/preprints202107.0664.v1

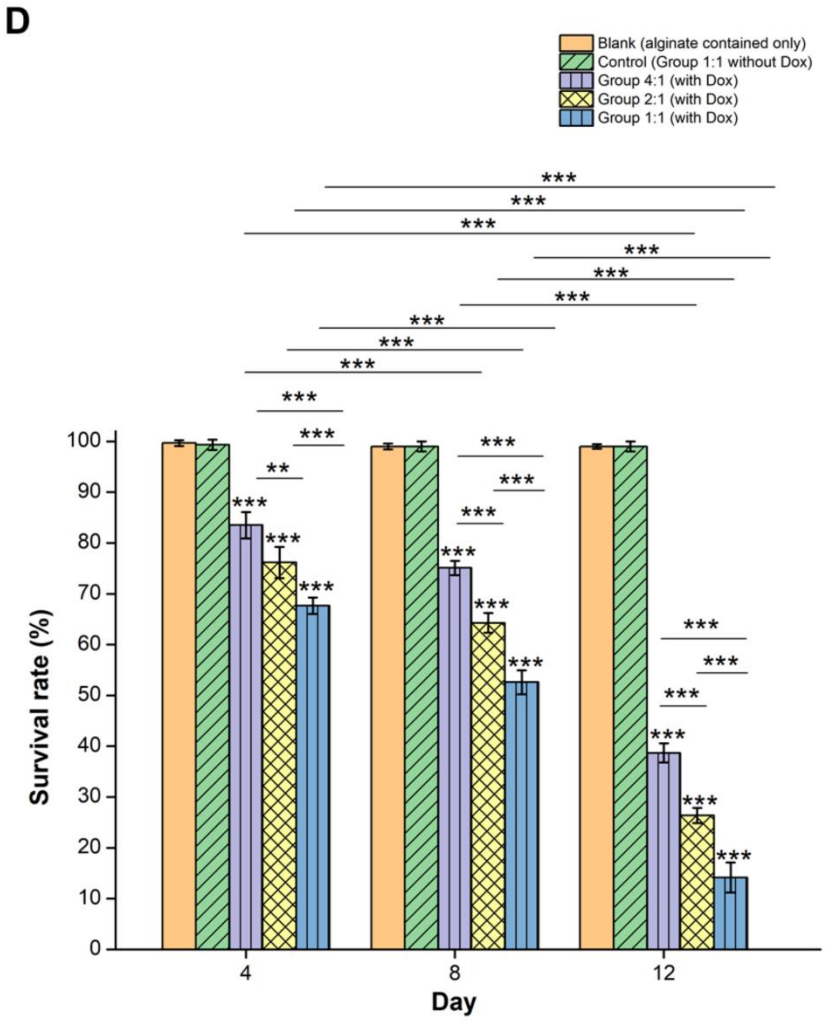

Figure 9. Treatments of Dox microspheres with relative high $NaHCO_3$ concentrations significantly reduced cell viabilities in two distinct HCC derived-cells, Huh-7 and Hep-3B, in vitro. An inverted microscope showed cell of **(A)** Huh-7 cells and **(B)** Hep-3B cells before and after treatments with blank (alginate only), control [Group 1:1 (alginate:$NaHCO_3$) without Dox, Group 4:1 with Dox, 2:1 with Dox and 1:1 with Dox, respectively, after treatments for 1, 2, 4, 8 and 12 day, scale bar = 200 μm. **(C, D)** In both cell lines, Dox microspheres with relative high $NaHCO_3$ concentrations steadily reduced cell viabilities at day 4, 8 and 12 after treatments compared to the control group. Within the same group, prolonged treatments from day 4 to day 12 decreased cell viabilities as well. Statistical significance: $^{**}p < 0.01$, $^{***}p < 0.001$.

4. Conclusions

Taken together, ultrasonic atomization was used to fabricate alginate microspheres. The

concentration of $CaCl_2$ and flow rate of the pump are critical parameters to produce calcium microspheres with an average Dv(50) ~ 39 μm. Among several groups with different alginate:$NaHCO_3$ ratios, flow rates were optimized in each group. Dox loaded efficiencies were correlated to encapsulation efficiencies across five groups with different alginate:$NaHCO_3$ ratios. Fourier spectrum showed the successful fabrication of alginate microspheres containing Dox and $NaHCO_3$, step-by-step. The surfaces are rough and porous in microspheres with higher $NaHCO_3$ concentrations. The Young's modulus and hardness reach highest in Group 1:1 (alginate:$NaHCO_3$). In vitro, swelling rates are higher across three groups with different alginate:$NaHCO_3$ ratios in pH 7.4 PBS compared to pH 6.5 PBS. Alginate microspheres containing Dox and relative high $NaHCO_3$ concentrations showed higher environmental pH values, Dox release rates in PBS and PBS containing 10% FBS, and significantly inhibited cell viabilities in two HCC-derived cells, Huh-7 and Hep-3B in vitro compared to those containing relative low $NaHCO_3$ concentrations. Incorporating $NaHCO_3$ in calcium alginate microspheres with Dox significantly decreased cell viabilities in distinct HCC-derived cells.

Supplementary Materials: The following are available online at XXX, Table S1: A 4 by 5 experiment was designed to identify the optimal combination(s) for the fabrication of calcium alginate microspheres. Table S2: Codes and levels of all parameters. Table S3: A total of 17 experiments were performed to detect the optimal parameters. Table S4: Comparison of the volume median diameters [Dv(50)] between different groups (alginate:$NaHCO_3$) with a specific flow rate. Table S5: Comparison of the swelling ratios between microspheres after the immersion into pH 6.5 PBS and pH 7.4 PBS from 0.5 to 24 h within each group with a specific alginate:$CaCl_2$ ratio. Table S6: Comparison of the swelling rates of microspheres between groups (with different alginate:NaHCO3 ratios) after the immersion into pH 6.5 PBS and pH 7.4 PBS from 0.5 to 24 h. Table S7: Comparison of the average pH values between microsphere in PBS and PBS containing 10% FBS in different groups with different alginate:$NaHCO_3$ ratios after the immersion from day 1 to day 22. Table S8: Comparison of the average pH values among microspheres with different alginate:$NaHCO_3$ ratios in PBS and PBS containing 10% FBS after the immersion from day 1 to day 22. Table S9: Comparison of the accumulated Dox release rates between microspheres in PBS and PBS containing 10% FBS in different groups (ratio = alginate:$NaHCO_3$) from day 1 to day 22 after immersion. Table S10: Comparison of the accumulated Dox release rates among

microspheres in PBS and PBS containing 10% FBS (ratio = alginate:$NaHCO_3$) from day 1 to day 22. Table S11: Model summary of multiple linear regression analysis used to evaluate the effects of Dox release amount (μg) and the environmental pH value on cell viabilities. Table S12: Analysis of variance (ANOVA) showed the regression, residual, F and *p* values after treatments with Dox/$NaHCO_3$ calcium alginate microspheres for 4, 8 and 12 days.

Author Contributions: Conceptualization, CT Pan, CY Yu and YL Shiue; Data curation, RS Yu and CJ Yang; Formal analysis, CJ Yang; Funding acquisition, CT Pan, ZH Wen and CY Yu; Investigation, RS Yu, CJ Yang, LR Chen, NY Chen and HY Ou; Methodology, CJ Yang, LR Chen, NY Chen and HY Ou; Project administration, CT Pan and YL Shiue; Resources, CT Pan, ZH Wen, HY Ou, CY Yu and YL Shiue; Software, LR Chen; Supervision, CY Yu; Writing – original draft, Yow-Ling Shiue.

Funding: This research was funded by the joined grant CMRPG8K0201 from Kaohsiung Chang Gung Memorial Hospital, and Chang Gung University College of Medicine, Kaohsiung, Taiwan and National Sun Yat-sen University and grant KAFGH_A_110006 from Kaohsiung Armed Forces General Hospital.

Institutional Review Board Statement: Not applicable.

Informed Consent Statement: Not applicable.

References

1. Couri, T.; Pillai, A. Goals and targets for personalized therapy for HCC. *Hepatol Int* **2019**, *13*, 125-137.
2. Llovet, J.M.; Real, M.I.; Montaña, X.; Planas, R.; Coll, S.; Aponte, J.; Ayuso, C.; Sala, M.; Muchart, J.; Solà, R.; et al. Arterial embolisation or chemoembolisation versus symptomatic treatment in patients with unresectable hepatocellular carcinoma: a randomised controlled trial. *Lancet* **2002**, *359*, 1734-1739.
3. Raoul, J.L.; Forner, A.; Bolondi, L.; Cheung, T.T.; Kloeckner, R.; de Baere, T. Updated use of TACE for hepatocellular carcinoma treatment: How and when to use it based on clinical evidence. *Cancer Treat Rev* **2019**, *72*, 28-36.
4. Lewis, A.L.; Holden, R.R. DC Bead embolic drug-eluting bead: clinical application in the locoregional treatment of tumours. *Expert opinion on drug delivery* **2011**, *8*, 153-

169.

5. Vaidya, S.; Tozer, K.R.; Chen, J. An overview of embolic agents. *Seminars in interventional radiology* **2008**, *25*, 204-215.
6. de Baere, T.; Plotkin, S.; Yu, R.; Sutter, A.; Wu, Y.; Cruise, G.M. An In Vitro Evaluation of Four Types of Drug-Eluting Microspheres Loaded with Doxorubicin. *J Vasc Interv Radiol* **2016**, *27*, 1425-1431.
7. Noh, S.Y.; Gwon, D.I.; Park, S.; Yang, W.J.; Chu, H.H.; Kim, J.W. Diaphragmatic weakness after transcatheter arterial chemoembolization of the right inferior phrenic artery for treatment of hepatocellular carcinoma: a comparison of outcomes after N-butyl cyanoacrylate versus gelatin sponge embolization. *Acta radiologica (Stockholm, Sweden : 1987)* **2020**, 284185120981771.
8. Kim, J.S.; Kwak, B.K.; Shim, H.J.; Lee, Y.C.; Baik, H.W.; Lee, M.J.; Han, S.M.; Son, S.H.; Kim, Y.B.; Tokura, S.; et al. Preparation of doxorubicin-containing chitosan microspheres for transcatheter arterial chemoembolization of hepatocellular carcinoma. *Journal of microencapsulation* **2007**, *24*, 408-419.
9. Zhang, J.; Han, J.; Zhang, X.; Jiang, J.; Xu, M.; Zhang, D.; Han, J. Polymeric nanoparticles based on chitooligosaccharide as drug carriers for co-delivery of all-trans-retinoic acid and paclitaxel. *Carbohydrate polymers* **2015**, *129*, 25-34.
10. Zeng, J.; Li, L.; Zhang, H.; Li, J.; Liu, L.; Zhou, G.; Du, Q.; Zheng, C.; Yang, X. Radiopaque and uniform alginate microspheres loaded with tantalum nanoparticles for real-time imaging during transcatheter arterial embolization. *Theranostics* **2018**, *8*, 4591-4600, doi:10.7150/thno.27379.
11. Pan, C.T.; Chien, S.T.; Chiang, T.C.; Yen, C.K.; Wang, S.Y.; Wen, Z.H.; Yu, C.Y.; Shiue, Y.L. Optimization of the spherical integrity for sustained-release alginate microcarriers-encapsulated doxorubicin by the Taguchi method. *Scientific reports* **2020**, *10*, 21758.
12. Chen, G.; Wei, R.; Huang, X.; Wang, F.; Chen, Z. Synthesis and assessment of sodium alginate-modified silk fibroin microspheres as potential hepatic arterial embolization agent. *International journal of biological macromolecules* **2020**, *155*, 1450-1459.
13. Becker, T.A.; Kipke, D.R.; Brandon, T. Calcium alginate gel: a biocompatible and mechanically stable polymer for endovascular embolization. *Journal of Biomedical Materials Research: An Official Journal of The Society for Biomaterials and The Japanese Society for Biomaterials* **2001**, *54*, 76-86.
14. Tønnesen, H.H.; Karlsen, J. Alginate in drug delivery systems. *Drug development and industrial pharmacy* **2002**, *28*, 621-630.
15. Guarino, V.; Caputo, T.; Altobelli, R.; Ambrosio, L. Degradation properties and metabolic activity of alginate and chitosan polyelectrolytes for drug delivery and tissue engineering applications. *AIMS Materials Science* **2015**.

16. Liu, D.; Wang, P.; Qi, X.; Zou, Q.; Zou, Y.; Hong, H. Pharmacokinetics of doxorubicin alginate microspheres and evaluation of its hepatic arterial embolization in vivo. *Yao xue xue bao= Acta pharmaceutica Sinica* **2006**, *41*, 778-783.
17. DeBerardinis, R.J.; Chandel, N.S. We need to talk about the Warburg effect. *Nat Metab* **2020**, *2*, 127-129.
18. Vaupel, P.; Schmidberger, H.; Mayer, A. The Warburg effect: essential part of metabolic reprogramming and central contributor to cancer progression. *International journal of radiation biology* **2019**, *95*, 912-919.
19. Vander Heiden, M.G.; Cantley, L.C.; Thompson, C.B. Understanding the Warburg effect: the metabolic requirements of cell proliferation. *Science* **2009**, *324*, 1029-1033.
20. Schwartz, L.; Seyfried, T.; Alfarouk, K.O.; Da Veiga Moreira, J.; Fais, S. Out of Warburg effect: An effective cancer treatment targeting the tumor specific metabolism and dysregulated pH. *Seminars in cancer biology* **2017**, *43*, 134-138, doi:10.1016/j.semcancer.2017.01.005.
21. Pérez-Tomás, R.; Pérez-Guillén, I. Lactate in the Tumor Microenvironment: An Essential Molecule in Cancer Progression and Treatment. *Cancers (Basel)* **2020**, *12*, doi:10.3390/cancers12113244.
22. Chao, M.; Wu, H.; Jin, K.; Li, B.; Wu, J.; Zhang, G.; Yang, G.; Hu, X. A nonrandomized cohort and a randomized study of local control of large hepatocarcinoma by targeting intratumoral lactic acidosis. *eLife* **2016**, *5*.
23. Chan, E.S.; Lee, B.B.; Ravindra, P.; Poncelet, D. Prediction models for shape and size of ca-alginate macrobeads produced through extrusion-dripping method. *J Colloid Interface Sci* **2009**, *338*, 63-72.
24. Castillo, E.; Ramirez, D.; Casas, L.; Lopez-Munguía, A. A two-phase method to produce gel beads. *Applied Biochemistry and Biotechnology* **1992**, *34*, 477.
25. Smrdel, P.; Bogataj, M.; Mrhar, A. The influence of selected parameters on the size and shape of alginate beads prepared by ionotropic gelation. *Sci Pharm* **2008**, *76*, 77-89.
26. Zhou, Z.; Liu, X.; Liu, Q. A comparative study of preparation of porous poly-L-lactide scaffolds using NaHCo3 and NaCl as porogen materials. *Journal of Macromolecular Science* **2008**, *47*, 2008.
27. Barba, A.A.; d'Amore, M.; Cascone, S.; Lamberti, G.; Titomanlio, G. Intensification of biopolymeric microparticles production by ultrasonic assisted atomization. *Chemical Engineering and Processing: Process Intensification* **2009**, *48*, 1477-1483.
28. Raoul, J.L.; Heresbach, D.; Bretagne, J.F.; Ferrer, D.B.; Duvauferrier, R.; Bourguet, P.; Messner, M.; Gosselin, M. Chemoembolization of hepatocellular carcinomas. A study of the biodistribution and pharmacokinetics of doxorubicin. *Cancer* **1992**, *70*, 585-590.

29. Kan, Z.; Wallace, S. Sinusoidal embolization: impact of iodized oil on hepatic microcirculation. *J Vasc Interv Radiol* **1994**, *5*, 881-886.
30. Lewis, A.L. DC Bead: a major development in the toolbox for the interventional oncologist. *Expert Rev Med Devices* **2009**, *6*, 389-400.
31. Obara, S.; Yamauchi, T.; Tsubokawa, N. Evaluation of the stimulus response of hydroxyapatite/ calcium alginate composite gels. *Polymer Journal* **2010**, *42*, 161-166.
32. Tong, Z.; Chen, Y.; Liu, Y.; Tong, L.; Chu, J.; Xiao, K.; Zhou, Z.; Dong, W.; Chu, X. Preparation, Characterization and Properties of Alginate/Poly(gamma-glutamic acid) Composite Microparticles. *Mar Drugs* **2017**, *15*.
33. Hazra, M.; Dasgupta Mandal, D.; Mandal, T.; Bhuniya, S.; Ghosh, M. Designing polymeric microparticulate drug delivery system for hydrophobic drug quercetin. *Saudi Pharm J* **2015**, *23*, 429-436.
34. Segale, L.; Giovannelli, L.; Mannina, P.; Pattarino, F. Calcium Alginate and Calcium Alginate-Chitosan Beads Containing Celecoxib Solubilized in a Self-Emulsifying Phase. *Scientifica (Cairo)* **2016**, *2016*, 5062706.
35. Bressac, B.; Galvin, K.M.; Liang, T.J.; Isselbacher, K.J.; Wands, J.R.; Ozturk, M. Abnormal structure and expression of p53 gene in human hepatocellular carcinoma. *Proceedings of the National Academy of Sciences of the United States of America* **1990**, *87*, 1973-1977.
36. Friedman, S.L.; Shaulian, E.; Littlewood, T.; Resnitzky, D.; Oren, M. Resistance to p53-mediated growth arrest and apoptosis in Hep 3B hepatoma cells. *Oncogene* **1997**, *15*, 63-70.